C. R. Mecanique 345 (2017) 137–152

Contents lists available at ScienceDirect

Comptes Rendus Mecanique

www.sciencedirect.com

Simulation-based conceptual design of an acoustic metamaterial with full band gap using an air-based 1-3 piezoelectric composite for ultrasonic noise control

Shahrokh Rezaei, Morteza Eskandari-Ghadi, Mohammad Rahimian *

School of Civil Engineering, College of Engineering, University of Tehran, P.O. Box: 4563-11155, Tehran, Iran

ARTICLE INFO

Article history:
Received 19 August 2016
Accepted 22 November 2016
Available online 15 December 2016

Keywords:
Phononic crystal
Acoustic band gaps
Passive control
Piezoelectricity
Vibration isolation
Ultrasonic noise control

ABSTRACT

This paper aims at proposing a novel type of acoustic metamaterials with complete band gap composed of piezoelectric rods with square array as inclusions embedded in an air background (matrix). A modified plane wave expansion method accompanied with the principles of the Bloch–Floquet method with electromechanical coupling effect and also impedance spectra are used to get a band frequency and to investigate the passband for the selected cut of piezoelectric rods. We investigate both the electromechanical coupling coefficient and mechanical quality factor and their dependency to passband and bandwidth, which depends on both the density and the wave impedance of the matrix and the inclusions (rods). The ratio of the volume of inclusion to the matrix is used to define the fill factor or the so-called inclusion ratio, to introduce the bandwidth as a function of that. Furthermore, the fabrication method is presented in this paper. The results make a suitable foundation for design purposes and may develop an inherently passive ultrasonic noise control. In addition, the results provide the required guidance for a simulation-based design of elastic wave filters or wave guide that might be useful in high-precision mechanical systems operated in certain frequency ranges and switches made of piezoelectric materials; they also propose a novel type of elastic metamaterials, which is independent of the wave direction and has an equal sensitivity in all directions in which it reacts omnidirectionally and mitigates the occupational noise exposure.

1. Introduction

Having industrialized the modern world, the literature and private studies have confirmed the adverse effects of industrial noise in the working environment on human hearing. Indeed, in high-frequency audiometry, i.e. 8–20 kHz, significant changes occur in the hearing threshold level [1]. Many countries (e.g., France and Germany) are working on assessing the harmfulness of occupational noise exposure and on amending the admissible values in the ultrasonic range [1]. France determines admissible values of ultrasonic noise and recommends limiting noise exposure in the high-frequency audible range (8–20 kHz) and the low-frequency ultrasonic range (20–50 kHz) [1]. Phononic crystals have analogue properties to photonic

* Corresponding author.
E-mail address: rahimian@ut.ac.ir (M. Rahimian).

http://dx.doi.org/10.1016/j.crme.2016.11.003
1631-0721/

Nomenclature

$\mathbf{G}$	The vectors of reciprocal lattice	$2\pi/\Lambda_{x_2}$	Normalized reciprocal lattice vector along x_2
$\mathbf{k}$	The "Bloch" wave vector	$\mathbf{U}(\mathbf{r},t)$	Generalized displacement or generalized stress vectors
f	Filling fraction ratio	$F(\mathbf{G})$	The structure function
r	The radius of cylindrical scattering material	c_{ijkl}	The elastic coefficients tensor
σ_{ij}	Cauchy stress tensor	ε_{ij}	Linear part of the elastic strain tensor
e_{ijk}	The piezoelectric coefficients	ω	Frequency
ρ	Material density	$\alpha(\mathbf{r})$	The Fourier component of arbitrary material constants
ϕ	Electric potential	u_i	Displacement vector
D_i	The electric displacement vector fields	J_1	The first kind Bessel function of first order
A_c	The Fourier component of arbitrary material constants	A_c	The area of the primitive unit cell
$\mathbf{A_G}$	The amplitude vector of the partial waves		
E_i	The electric field		

crystals [2–4]. Hence, shortly after starting the research on photonic band gaps, where the band gaps or stop bands are observed for electron waves in semiconductors; the idea has been extended to both electromagnetic waves in photonic crystals and elastic waves in phononic crystals [5]. These types of meta-materials, constituted by a periodic repetition of two different materials, can either show absolute band gaps in their transmission spectra [6,7], where the elastic waves do not propagate at some frequencies, or dictate the modes that are allowed to be propagated in the material. Moreover, these types of materials can decrease the velocity of the elastic waves and even represent negative refraction [8]. This capability offers the idea of constructing new meta-materials with special performance for vibration control [9] or producing acoustic shield with applications in designing acoustic filters, wave guides, mirrors, and wave transducers. Similarly, several phenomena such as guiding [10–12], bending [13,14], filtering [15,12], demultiplexing [3], and super lenses for acoustic waves [16] have been predicted so far. On the other hand, phononic crystals can tailor the allowed modes and their wave speeds inside the material in such a way that the frequencies of various material losses subjected to different regimes is to be matched with the density of some states and frequencies of some modes in order to provide enhanced energy absorption [5]. Since mechanical waves propagate in a solid in the form of both longitudinal and transverse waves, a designated structure with complete phononic filters might have band gaps for both waves in the same frequency region [17].

The geometry and composition characteristics of phononic filters play essential roles in showing forbidden gaps of wave propagation in these filters, regardless of wave polarization and propagation directions. However, the larger the bandwidth for these forbidden zones, the more the applications for phononic filters. Actually, the bandwidth for this forbidden zone is a key factor for some purposes, e.g., for vibration control at specific frequencies. Some researchers have tried to enlarge the width of band gaps (e.g., see [18]). They showed that the width of band gaps may be determined by the contrast of elastic constants, the inclusion (filling) volume fraction, and the lattice of the constructed parts. Changing either the geometry or the elastic characteristics of the constitutive materials through external stimuli such as wave propagation causes the band structure of phononic crystal to be adjusted to a specific range of frequencies, and thus, represents either a partial or a full band gap.

Geometry design of phononic crystals with its inclusions and of matrices with tunable band gaps is an interesting but challenging issue. The ability to tune the band gaps leads to make both non-absorbing mirrors for elastic waves and vibration-free cavities, which might be useful in high-precision mechanical systems [19] operated in certain frequency ranges. Thus, a phononic crystal may be designated in such a way that it can be adjusted in a desired band gap configuration.

Some functional materials such as thermally activated shape memory alloys, electro-rheological materials, dielectric elastomeric layers, and either magneto-elastic or magneto-electro-elastic materials have been selected to be used to capture a tunable passband and stop band in phononic crystals with higher efficiency [20–24]. Representing a full band gap for phononic crystals could lead to improve the design of transducers and vibration controllers.

The high electromechanical coupling factor and low wave impedance at piezoelectric materials [25,26] stimulate the piezoelectric-based phononic crystal developments. Moreover, piezoelectric materials have some unique properties as compared with other tunable materials such as shape memory alloys and electro-rheological materials, which make the piezoelectric materials to be highly accurate in the control of displacement, quick response, and to reduce the device size strongly [27]. But, since the piezoelectric substrate is not isotropic, they allow bulk waves to travel with different speeds in different directions. These phenomena cause piezoelectric crystals to be configured in such a way that the full band gap will result. A key note is that the velocities of bulk wave propagation or the slowness of surfaces in anisotropic piezoelectric materials have directional dependency [28]. Since the band gap property depends on both geometry and wave impedance, there is a need to investigate the effect of these parameters accurately to catch suitable configurations for inclusions to reach the desired performance.

Simulation-based design is a breakthrough toward complex systems, where the electromechanical coupling factor, the filling fraction effect, the impedance spectra and numerical challenges shall be taken into account for an accurate design and to avoid both a high cost of experiment and the cost induced by trial and error set-ups.

There can be three perpendicular polarization planes for elastic waves in piezoelectric materials and three different body waves, namely longitudinal, in-the-plane transverse (shear), and out-of-the-plane transverse waves can propagate in each plane [29]. Thus, piezoelectric based metamaterials must prohibit propagating all types of waves in all directions in order to have a structure for a full band gap. Propagating elastic waves in a medium is usually described by a dispersion relationship between frequency and wave vector. There exist some tools for band diagram prediction, which are very complicated in inhomogeneous materials. However, there are also various methods to obtain high-quality dispersion curves, one of which is Plane Wave Expansion Method (PWEM) [30]. Although this method has been developed for electromagnetic wave, it is a powerful method even for calculating the dispersion relationships for both acoustic and elastic waves, it fails in some cases where the material contrast between inclusions and matrix is high. In this context, an extremely large number of Fourier's components are needed to ensure enough accuracy. Here the principle of the Bloch–Floquet method [31] is carried out to calculate the wave modes and group velocities, even for complex propagation constants. Recent developments in piezoelectric-based smart materials (e.g., one-dimensional phononic crystal) [32] or piezoelectric-based vibration control [33] show that vibration control with an enough large band gap through suitable rod materials is possible; however, in the low-frequency ultrasonic range, the passive vibration control or acoustic shield is very difficult. Thus, the vibroacoustic control or vibration isolation with complete band gap, where no wave propagates, will have excellent performance and stimulate developments in practical purposes, and it will be easy to use, especially for occupational noise exposure mitigation.

In this article, a novel type of phononic crystal in the form of a meta-composite with complete band gap and inherently passive behavior, which consists of a cylindrical piezoelectric material with a square array as an inclusion embedded in an air background is proposed. The rods in this phononic crystal are arranged according to a special configuration, and a modified plane wave expansion method and the principles of the Bloch–Floquet method accompanied with electromechanically coupling effect are employed to get the band structure and to study the pass bands. We separately investigate the dependency of passband and of its bandwidth on the density of the proposed phononic crystal and on the wave impedance of background and inclusion. In addition, the effects of the inclusion ratio defined as the volume ratio of the inclusion and the whole composite on the performance of the band gap and piezoelectric material are studied. The results make a suitable concrete foundation for the development of a passive vibration or ultrasonic noise controller that will be used in the design of wave filters and switches made of a piezoelectric-based meta-composite. The results may also be useful for making acoustic noise control devices. Additionally, these types of meta-composite materials have full band gap properties that can be used for making a standalone vibration isolator. The full band gap property improves the vibroacoustic comfort and the general performance of devices that reduce industrial noise in working environments.

This paper consists of seven sections, as follows.

Section 2 introduces the candidate rod-based piezoelectric metamaterials, and the associated acoustic wave velocities in cases with and without electromechanical coupling, and the figure-of-merit effects. Section 3 introduces modified the Plane-Wave Expansion Method (PWEM) associated with the "Bloch–Floquet" method, where electromechanical coupling effects, mechanical quality factors, as well as impedance spectra of piezoelectric materials are taken into account for designing the acoustic band gap. In Section 4, the key parameters with the associated results are documented. Section 5 offers the fabrication method, and finally the analysis of the results and of the conclusions is presented in Sections 6 and 7, respectively.

2. Determining the acoustic wave velocity in the candidate piezoelectric material and the figure of merit

The high accuracy in the control of displacement, quick response, and especially strong reduction of the size of the device made by piezoelectric materials are motivations toward piezoelectric-based metamaterials. Since the band gap property is related to the wave contrast between two different media, a maximizing band-gap-width strategy leads to increase the acoustic wave velocity contrast between two media. On the other hand, as the piezoelectric substrate is not isotropic, the bulk waves travel at different speeds in different directions. Here, the ranges of acoustic wave velocity that the rod can support are investigated by considering the effects of both anisotropy and electromechanical coupling as the first step. To do this, lithium niobate with strong coupling [34] is selected to investigate the effect of piezoelectric rods on the band gap. The inherent high purity of "lithium niobate" makes it a candidate for acoustic wave applications. Due to its chemical insensitivity, etching techniques are suitable for fabrication, which allows periodic structures with reasonable size and filling fraction to be achieved. Furthermore, these techniques are compatible with acoustic wave guides where fabricating a two-dimensional phononic crystal will be possible. The acoustic waves are confined in three dimensions in this crystal. The rods properties can be found here.[1]

[1] http://www.efunda.com/materials/piezo/material_data/matdata_output.cfm?Material_ID=LiNbO.

Piezoelectricity is described mathematically within a material constitutive equation, which defines how the stress tensor (σ), the strain tensor (S), the charge-density displacement vector (D), and the electric field vector (E) interact in piezoelectric materials.

The piezoelectric constitutive law (in strain–charge form) is:

$$S = s_E \cdot \sigma + d^{\mathrm{t}} \cdot E \tag{1}$$

$$D = d \cdot \sigma + \varepsilon_T \cdot E \tag{2}$$

The matrix d contains the piezoelectric coefficients for the material, and it appears twice in the constitutive equation (the superscript "t" stands for the **transpose** of the **matrix**). In addition, s_E and ε_T are the compliance matrix and permeability of the piezoelectric material. The compliance matrix, piezoelectric coupling and the relative permittivity for the lithium niobate material are respectively given as:

$$s_E = \begin{pmatrix} 5.78 & -1.01 & -1.47 & -1.02 & 0 & 0 \\ -1.01 & 5.78 & -1.47 & 1.02 & 0 & 0 \\ -1.47 & -1.47 & 5.02 & 0 & 0 & 0 \\ -1.02 & 1.02 & 0 & 17 & 0 & 0 \\ 0 & 0 & 0 & 0 & 17 & -2.04 \\ 0 & 0 & 0 & 0 & -2.04 & 13.6 \end{pmatrix} \times 10^{-12}\ \frac{\mathrm{m}^2}{\mathrm{N}} \tag{3}$$

$$d = \begin{pmatrix} 0 & 0 & 0 & 0 & 68 & -42 \\ -21 & 21 & 0 & 68 & 0 & 0 \\ -1 & -1 & 6 & 0 & 0 & 0 \end{pmatrix} \times 10^{-12}\ \frac{\mathrm{C}}{\mathrm{N}} \tag{4}$$

$$\frac{\varepsilon_T}{\varepsilon_0} = \begin{pmatrix} 84 & 0 & 0 \\ 0 & 84 & 0 \\ 0 & 0 & 30 \end{pmatrix}, \qquad \varepsilon_0 = 8.854 \times 10^{-12}\ \frac{\mathrm{F}}{\mathrm{m}} \tag{5}$$

The acousto-optic figure of merit (FOM) indicates the ideal coupling orientation maximizing the refractive index change due to an acoustic signal. The figure of merit is calculated as:

$$FOM = \frac{n^6 p^2}{\rho v^3} \tag{6}$$

where n is the refractive index, p is the elastic constant, ρ is the density, and v is the velocity. A method for the directional dependent refractive index and FOM is presented by McIntosh [35].

In Fig. 1, using Mathematica® code, the acousto-optic figure of merit for the Y-cut lithium niobate is plotted.

The crystal cut (the cuts are labeled based on the perpendicular plane on them) determines the properties of the crystal and the affected mode of vibration, frequency stability, acoustic wave velocity, aging and other parameters. Therefore, from a practical point of view, the crystal cut is significant.

Based on the modified Christoffel's equation, [37], dominant modes of acoustic wave velocities in a piezoelectric rod with and without coupling effects were plotted for the selected crystal cut by using Mathematica® code.

As seen in Figs. 2 (a), (b), (c), the anisotropy and coupling effect on the acoustic wave velocities depend on specific 3D velocity distribution induced by the coupling, and the crystal cut. These velocities are denoted by longitudinal, in plane and out of plane wave velocities. This is one of the key parameters for design purposes. The large gaps are the results of high contrast in both velocities and mass densities [38]. In this regard, the cylinders are made of the high velocity materials for composite systems presenting very large complete acoustic gaps. Therefore, the velocity ranges supported by rods are important (Appendix A). These figures represent the longitudinal, in plane and out of plane wave velocities. They signify the correlation between anisotropy, electromechanical coupling effect, and wave velocity, and represent the acoustic wave velocity ranges that rod can support. Since the wave velocity ratio between the two media at metamaterials is important for desirable full or partial band gap, these results are critical to choose the suitable inclusion and wafer. The low contrast may lead to partial or no band gap. To cover the full band gap, all acoustic wave velocities that can be supported by any type of the selected piezoelectric should be considered to lead the full band gap. The air is selected in order to enhance the efficiency and performance of metamaterials, especially in specific frequency regime. In this way, the density and the acoustic wave contrast is increased, and the phononic crystal size is decreased (Appendix A). When scattering occurs coherently from equally spaced layers in a phononic crystal, the band gap opens up at the border of the first Brillouin zone. Although the dispersion in the vicinity of the band gap will be modified, the center frequency of the band gap is approximately given by assuming linear dispersion based on the center frequency of a Bragg band gap, ($f_c \approx \frac{v}{2a}$) where "v" is the velocity at host and "a" is the lattice parameter [39]. Based on this approximation, the acoustic wave velocity at host has direct effect on center frequency of a Bragg band gap. Therefore, by increasing the wave velocity at host, the frequency band gap is likely changed to higher frequency range. The acoustic wave velocity at air is assumed as 343 m/s.

In summary, elastic metamaterial including lithium niobate embedded in honeycomb skeleton (for support) with air gap was proposed to mitigate the noise at ultrasonic range.

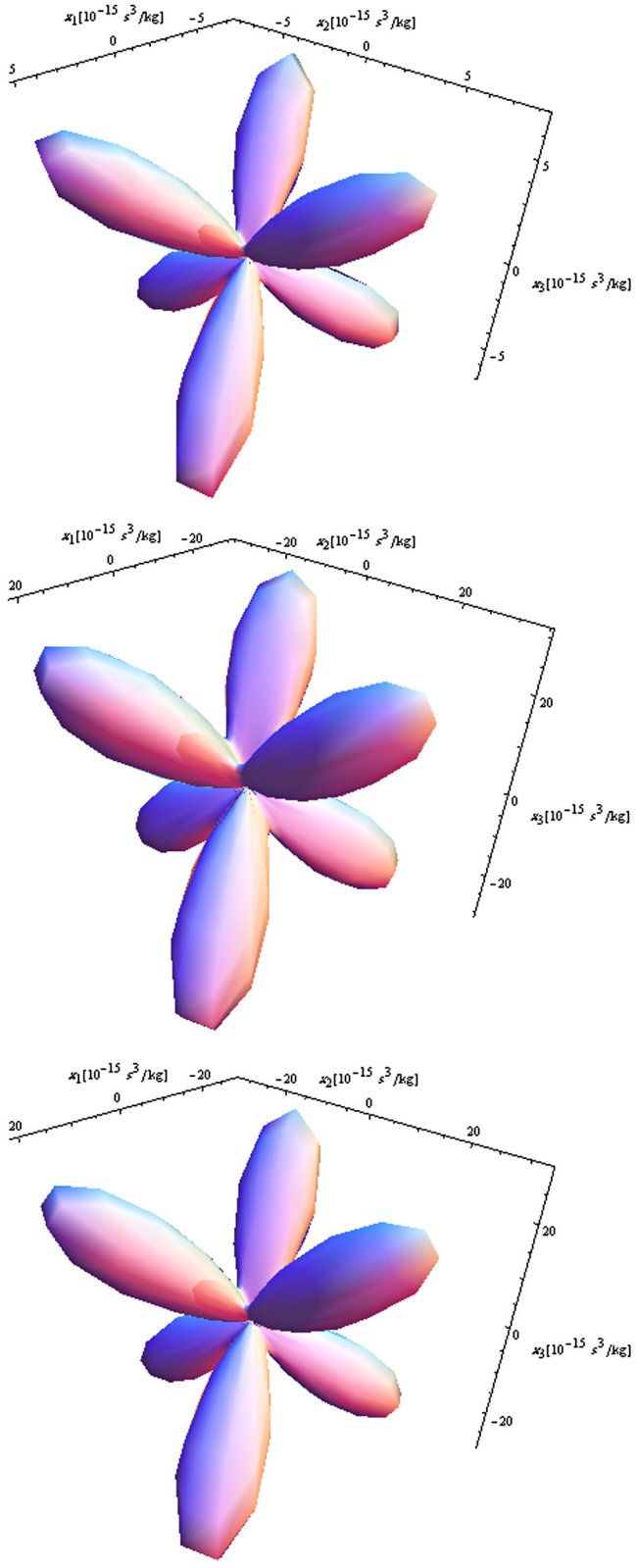

Fig. 1. The figure of merit for longitudinal, horizontal transversely, and vertical transversely wave respectively for Y-cut lithium niobate [36].

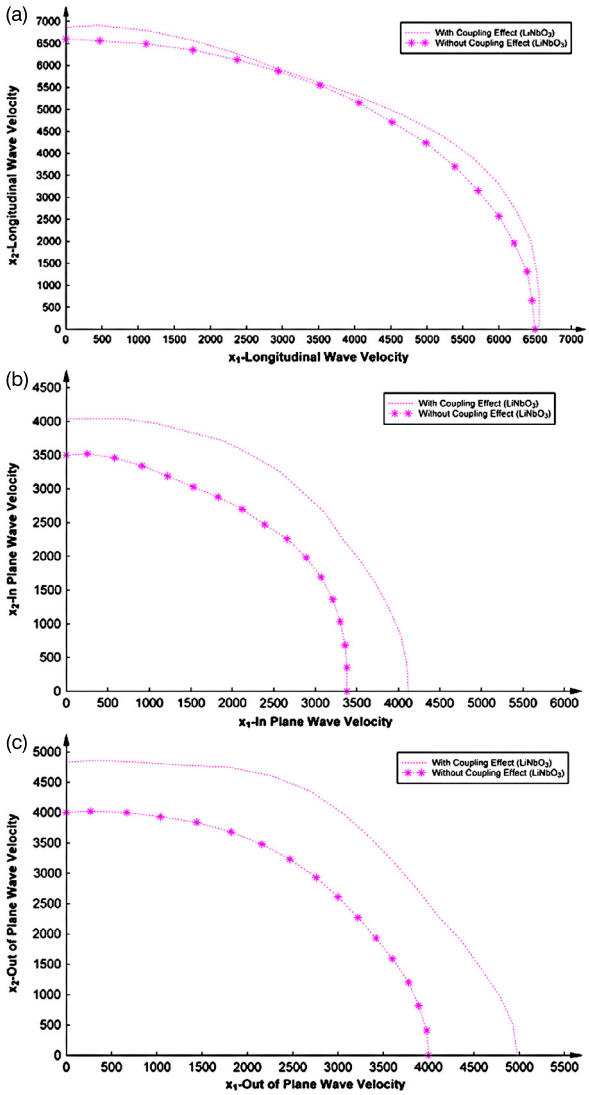

Fig. 2. (a), (b) and (c) represent the wave velocity of "Y-cut" wafers, denoted by longitudinal, in plane and out of the plane, for lithium niobate with and without electromechanical coupling effect.

3. Modeling a phononic crystal

The model considered here is a periodic two-dimensional system of cylindrical rods that play as scattering materials (Fig. 3), infinite long in the X_3-direction embedded in honeycomb skeleton with air gap. By this model, we are able to calculate the band structure for the propagation of plane waves traveling through this structure. The depth of the cylinders sets up a certain wavelength so that any wave with wavelength smaller than the depth of the cylinder sees the cylinders as infinitely long obstacles as far as the scattering process is concerned [40]. This subject will be shown by impedance spectra of piezoelectric materials at Section 3.2. The distance between cylindrical scattering materials is called the lattice parameter and is denoted by Λ_{x_1} along x_1 and Λ_{x_2} along x_2, while the radius of the cylindrical scattering material is denoted by r. The lattice parameter along x_1 and x_2 is here assumed to be equal to $\Lambda_{x_1} = \Lambda_{x_2} = \Lambda_0$. The filling fraction, f, is defined as the ratio of the scattered area to the area of unit cell, and is expressed as $f = \pi(r/\Lambda_0)^2$ for the circular scatters at square array (Fig. 4).

3.1. The Bloch form of the PWEM

Assuming a Cartesian coordinate system as a reference, the constitutive equations for a piezoelectricity with the equation of motion and Poisson's condition at dielectric media were given by Wilm et al. [42];

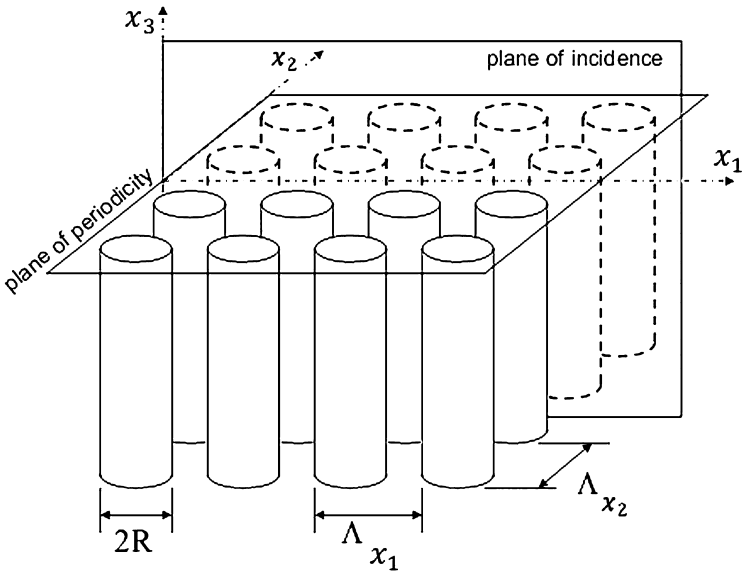

Fig. 3. A square-lattice, two-dimensional phononic crystal, consisting of cylindrical piezoelectric rods embedded in an air background.

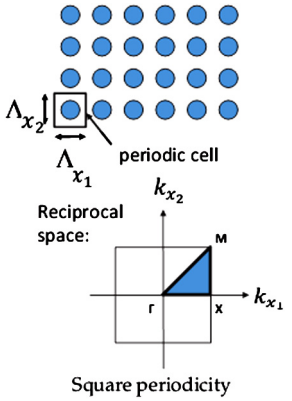

Fig. 4. 2D periodic arrangements and the associated first Brillouin zones. The corresponding first irreducible Brillouin zone where ΓX and ΓM are related to the $(1,0)$ and the $(1,1)$ direction, respectively; XM is the variation wave vector from $(1,0)$ to $(1,1)$ on the side of it. Adopted from © 2012 Antos R., Veis M. Originally published in [41] under CC BY 3.0 license. Available in: http://dx.doi.org/10.5772/34679.

$$\sigma_{ij} = c_{ijkl}\varepsilon_{kl} + e_{kij}\frac{\partial\phi}{\partial x_k} \tag{7}$$

$$D_k = e_{kij}\varepsilon_{ij} - \varepsilon_{ki}\frac{\partial\phi}{\partial x_i} \tag{8}$$

$$\rho\frac{\partial^2 u_j}{\partial t^2} = \sigma_{ij,i} \tag{9}$$

$$D_{i,i} = 0 \tag{10}$$

where the summation convention has been employed and $\sigma_{ij}(x_1, x_2, x_3, t)$ is the Cauchy stress tensor, $\varepsilon_{ij}(x_1, x_2, x_3, t)$ the linear part of the elastic strain tensor, and $D_i(x_1, x_2, x_3, t)$ is the electric displacement vector field. In addition, c_{ijkl} is the elastic coefficient, and e_{ijk} is the piezoelectric coefficient. In this paper, all the material coefficients are considered as being dependent on (x_1, x_2) and independent of x_3. The elastic strain tensor, ε_{ij}, is expressed in terms of displacement vector u_i as

$$\varepsilon_{ij} = \frac{1}{2}\left(\frac{\partial u_i}{\partial x_j} + \frac{\partial u_j}{\partial x_i}\right) \tag{11}$$

By the quasi-static approximation, the electric field may be expressed as the gradient of an electric potential $\phi(x_1, x_2, x_3)$ as

$$E_i = -\frac{\partial\phi}{\partial x_i} = -\phi_{,i} \tag{12}$$

The PWEM is a commonly used numerical technique to calculate the band structures for photonic crystals [43,39,44,45]. The PWEM can be applied to a phononic crystal with any shape of scattering; however, only infinite arrays can be modeled [46]. According to the Bloch–Floquet theorem, all fields in a periodic solid such as displacements and stresses can be expanded as infinite series [42,47].

$$h(\mathbf{r},t)=\sum_{\mathbf{G}}h_{\mathbf{G}}(\omega,\mathbf{k})\exp\left(\mathrm{j}(\omega t-\mathbf{k}\cdot\mathbf{r}-\mathbf{G}\cdot\mathbf{r})\right) \tag{13}$$

where h stands for either the displacements, or the stresses, or the electric potential, or the electric displacements, or the acoustic pressure field, $\mathrm{j}=\sqrt{-1}$, $\mathbf{r}=(x_1,x_2,x_3)^{\mathrm{T}}$. The superscript "T" is transposition, and the vectors of reciprocal lattice are

$$\mathbf{G}(m_1,m_2)=(2\pi m_1/a_1,2\pi m_2/a_2,0)^{\mathrm{T}}=(2\pi/\Lambda_{x_1},2\pi/\Lambda_{x_2},0)$$

which means that the set of all wave vectors $\mathbf{G}$ that give plane waves $\mathrm{e}^{\mathrm{j}\mathbf{G}\cdot\mathbf{r}}$ with the periodicity of the lattice and the $\mathbf{G}$-vectors correspond to the reciprocal lattice points. Here, $2\pi/\Lambda_{x_1}$ and $2\pi/\Lambda_{x_2}$, are the normalized reciprocal lattice vectors and are assumed to be periodic with a period of Λ_{x_j} along the x_j-axes [41]. In this expression, $\mathbf{k}$ is the "Bloch" wave vector and in a special case $a_1=a_2=a$, where a is lattice constant with m_1 and m_2 integers.

The main part of the PWEM is to expand the system functions such as density, speeds, and wave functions by plane waves that exist in the wave equation in the form of Fourier series in terms of x_1, x_2 and x_3 as:

$$\alpha(\mathbf{r})=\sum_{\mathbf{G}}\alpha_{\mathbf{G}}\mathrm{e}^{-\mathrm{j}\mathbf{G}\cdot\mathbf{r}} \tag{14}$$

where $\alpha(\mathbf{r})$ is the Fourier component of material constants including the material density, elasticity, piezoelectric, and dielectric tensors for the periodic structure, which depend on the position or

$$\alpha=\{\rho,c_{ijkl},e_{ijk},\varepsilon_{ij}\}$$

i.e.

$$\rho(\mathbf{r})=\sum_{\mathbf{G}}\mathrm{e}^{\mathrm{j}\mathbf{G}\cdot\mathbf{r}}\rho_{\mathbf{G}} \tag{15}$$

$$c_{ijkl}(\mathbf{r})=\sum_{\mathbf{G}}\mathrm{e}^{\mathrm{j}\mathbf{G}\cdot\mathbf{r}}{c_{\mathbf{G}}}^{ijkl} \tag{16}$$

The Fourier harmonics $\alpha_{\mathbf{G}}$ are calculated for various scattering materials and lattice geometries [22,42,48] and, the sum is taken only over the reciprocal lattice points. One may write $\alpha_{\mathbf{G}}$ as follows

$$\begin{aligned}&\alpha_{\mathbf{G}}=\alpha_{\mathbf{G}I}f+\alpha_{\mathbf{G}M}(1-f)\quad\text{when}\quad\mathbf{G}=0\\&\alpha_{\mathbf{G}}=(\alpha_{\mathbf{G}I}-\alpha_{\mathbf{G}M})F(\mathbf{G})\qquad\text{when}\quad\mathbf{G}\neq0\end{aligned} \tag{17}$$

where $\alpha_{\mathbf{G}I}$ and $\alpha_{\mathbf{G}M}$ stand for Fourier harmonics for the inclusion (cylindrical rod) and matrix (substrate). In addition, f is the area filling fraction, which is defined as the cross sectional area of a cylinder relative to a unit-cell area. As mentioned earlier, the subscripts I and M represent the inclusion and matrix, respectively. $F(\mathbf{G})$ in (17) is called the structure function defined as follows:

$$F(\mathbf{G})=A_{\mathrm{c}}^{-1}\int_{A_{\mathrm{c}}}\mathrm{d}^2\mathbf{r}\mathrm{e}^{-\mathrm{j}\mathbf{G}\cdot\mathbf{r}} \tag{18}$$

i.e.

$$\rho_{\mathbf{G}}=A_{\mathrm{c}}^{-1}\int_{A_{\mathrm{c}}}\mathrm{d}^2\mathbf{r}\rho(\mathbf{r})\mathrm{e}^{-\mathrm{j}\mathbf{G}\cdot\mathbf{r}} \tag{19}$$

$${c^{ijkl}}_{\mathbf{G}}=A_{\mathrm{c}}^{-1}\int_{A_{\mathrm{c}}}\mathrm{d}^2\mathbf{r}c^{ijkl}(\mathbf{r})\mathrm{e}^{-\mathrm{j}\mathbf{G}\cdot\mathbf{r}} \tag{20}$$

where A_{c} is the cross section area of the filling structure or the area of the primitive unit cell of a two-dimensional phononic structure. The proposed system consists of piezoelectric rods with square array and circular cross-section with air-gap material, which results in the following structure function factors for circular scatter [39]:

$$F_G=2f\frac{J_1(\mathbf{G}r_0)}{\mathbf{G}r_0},\quad 0\le f=\pi\frac{r_0^2}{a^2}\le\frac{\pi}{4} \tag{21}$$

where J_1 is the first-kind Bessel function of the first order. In each case, the maximum value of the filling fraction f corresponds to the close packing of the rods in the matrix. The irreducible part of the Brillouin zone of a square lattice is shown in Fig. 4.

The square lattice configuration has a reciprocal lattice vector defined in the PWE method as:

$$\mathbf{G} = \left(\frac{2\pi}{a}\right)(n_1 x_1 + n_2 x_2) \tag{22}$$

Using the Bloch theorem and expanding the unknown fields $\mathbf{u}(\mathbf{r}, t)$ in Fourier series with respect to the 2D reciprocal lattice vectors (RLVs), we have as follows:

$$\mathbf{u}(\mathbf{r}, t) = \sum_{\mathbf{G}} e^{jkx_1 - j\omega t}\left(e^{j\mathbf{G}x_1}\mathbf{A}_{\mathbf{G}} e^{jk_3 x_3}\right) \tag{23}$$

Here, $\mathbf{k} = (k_1, k_2)$ is the Bloch wave vector, ω is the frequency, k_3 is the wave number of the partial waves along the x_3-axis, and $\mathbf{A}_{\mathbf{G}} = (A^1_{\mathbf{G}}, A^2_{\mathbf{G}}, A^3_{\mathbf{G}})$ is the amplitude vector of the partial waves. If the component of the wave vector k_3 equals zero, the above equation degenerates into the vector filed of a bulk elastic wave.

One can define either a generalized displacement field $\{u^{x_1}_{\mathbf{G}}, u^{x_2}_{\mathbf{G}}, u^{x_3}_{\mathbf{G}}, \varphi_{\mathbf{G}}\}^{\mathrm{T}}$, in which $\varphi_{\mathbf{G}}$ represents the electrical potential or generalized stress vectors $\{\sigma^{x_1}_G, \sigma^{x_2}_G, \sigma^{x_3}_G, D_G\}^{\mathrm{T}}$ where D_G represents the electrical displacement field. If one denotes either of these vectors by $\mathbf{U}$, then one may write

$$\begin{aligned} \mathbf{U}_1 &= \{u^{x_1}_{\mathbf{G}}, u^{x_2}_{\mathbf{G}}, u^{x_3}_{\mathbf{G}}, \varphi_{\mathbf{G}}\}^{\mathrm{T}} \\ \mathbf{U}_2 &= \{\sigma^{x_1}_{\mathbf{G}}, \sigma^{x_2}_{\mathbf{G}}, \sigma^{x_3}_{\mathbf{G}}, D_{\mathbf{G}}\}^{\mathrm{T}} \end{aligned} \tag{24}$$

Upon utilizing the Bloch theorem and expanding this generalized displacement or generalized stress vector, $\mathbf{U}(\mathbf{r}, t)$, in Fourier series, and expanding the system functions such as density and the associated physical properties tensor and substitute both of them into the differential equations of motion in the absence of body forces, the generalized eigenvalue equation is obtained:

$$\omega^2 \mathbf{R}\mathbf{U} = \mathbf{Q}\mathbf{U} \tag{25}$$

where $\mathbf{R}$ and $\mathbf{Q}$ are two different $4N \times 4N$ matrices that are functions of $\mathbf{k}$, $\mathbf{G}$, $\mathbf{G}'$, the material constants and the filling fraction. This equation defines a generalized eigenvalue problem that can be solved for ω^2 as a function of $\mathbf{k}$ to obtain the band structure of the elastic waves where the electromechanical coupling effects without external charge are considered.

Since the density contrast of piezoelectric rods and air is large, the shear stress and transverse waves inside the rods will not have significant contribution to the scattering of acoustic waves in the background, so the modified PWE method is acceptable, and thus the acoustic wave pressure field rather than the displacement is used to get the corresponding band gap for this system. In addition, the acoustic wave pressure field has Bloch form. Thus, the secular equation that gives the dispersion relation between the frequency and the wave vector for the acoustic pressure field by applying the "Bloch theorem" is:

$$-\det[\Gamma_{(\mathbf{G})\cdot(\tilde{\mathbf{G}}')}] = \det\left[\alpha\left((\tilde{\mathbf{G}}) - (\tilde{\mathbf{G}}')\right)\left((\tilde{\mathbf{k}}) + (\tilde{\mathbf{G}})\right)\cdot\left((\tilde{\mathbf{k}}) + (\tilde{\mathbf{G}}')\right) - \beta\left((\tilde{\mathbf{G}}) - (\tilde{\mathbf{G}}')\right)\omega^2\right]_{(\tilde{\mathbf{G}})\cdot(\tilde{\mathbf{G}}')} = 0 \tag{26}$$

where $(\tilde{\mathbf{k}})$ is the Bloch wave vector, $\omega(k)$ is the frequency, and $(\tilde{\mathbf{G}})$ is the reciprocal lattice vector. $\alpha(\tilde{\mathbf{G}})$ and $\beta(\tilde{\mathbf{G}})$ are determined from an inverse Fourier transform and are related to the material property in characteristic wave equation.

3.2. Impedance spectra of piezoelectric rod and performance evaluation of piezoelectric materials

An applied electric field causes an induced strain in the piezoelectric material (i.e. converse piezoelectric effect), so the equivalent impedance of the piezoelectric rods will change along with the excitation frequency.

The electromechanical coupling effect coefficient in piezoelectric materials (an index for the energy conversion between electrical energy and acoustic energy) and mechanical quality factor (an index for energy wastage in form of heat resulted from internal friction when the PZT resonates) are key elements to evaluate the piezoelectric performance where the former is a function of series and parallel resonant frequencies that are calculated by using impedance spectra (ANSI/IEEE STD 176-1987), and the latter depends on the piezoelectric volume fraction.

Since the PZT cross-section affects the thickness and lateral vibration mode, long and thin piezoelectric materials shall be practically selected to limit the thickness vibration mode.

The thickness of the sensitive element shall be selected to ensure the center frequency of its coupled transducer.

The impedance spectrum of piezoelectric material is as follows:

$$\begin{aligned} Z(f) &= \frac{t/\mathrm{i}2\pi f \varepsilon_{33} w l}{1 - (k^l_{31})^2\left(1 - \frac{\tan(\pi f/2f_s)}{\pi f/2f_s}\right)} \\ \left(k^l_{31}\right)^2 &= d^2_{31}/\varepsilon_{33} s^E_{11} \end{aligned} \tag{27}$$

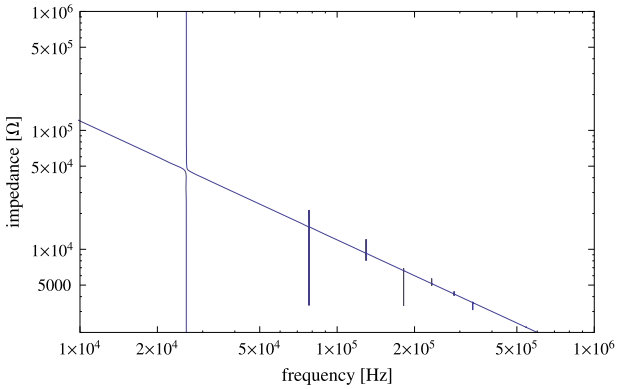

Fig. 5. The impedance spectrum of lithium niobate, where length = 100 mm, width = 0.5 mm, and thickness = 0.1 mm [49].

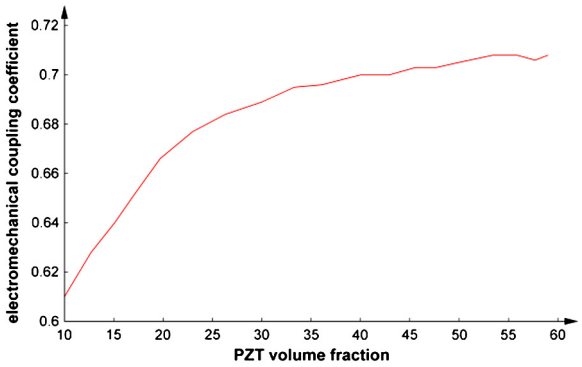

Fig. 6. The PZT volume fraction in terms of electromechanical coupling coefficient.

Using Mathematica®, the impedance spectrum of a piezoelectric rod was calculated (Fig. 5). Spikes in the spectrum indicate the locations of resonances. The frequency where the impedance is at a minimum is considered a resonance, and the frequency where a maximum occurs is considered anti-resonance. The lowest frequency spike is the fundamental resonance, and the higher spikes are the harmonics that occur at odd multiples of the fundamental resonance.

The impedance spectrum of piezoelectric rod is an index for the practical selection of piezoelectric materials dimensions where the electromechanical coupling coefficient and mechanical quality factor are considered simultaneously.

Based on the impedance spectrum of piezoelectric materials, the electromechanical coupling coefficient and the mechanical quality factor are determined as follows, respectively:

$$E.C.C. = \frac{\pi}{2}\frac{f_s}{f_p}\tan\left(\frac{\pi}{2} - \frac{f_p - f_s}{f_p}\right) \tag{28}$$

where f_s is the series resonant frequency and f_p is the parallel resonant frequency.

$$Q_m = \frac{f_p^2}{2\pi f_s |Z| C^{\mathrm{T}} (f_p^2 - f_s^2)} \tag{29}$$

where $|Z|$ and C^{T} are the minimum resonant impedance and free capacitance, respectively. The electromechanical coupling coefficient and the mechanical quality factor in terms of filling ratio are displayed in Figs. 6 and 7.

4. Numerical analysis

In this section, the numerical analysis of band-gap structures is presented to show the effect of piezoelectric rods or inclusions on longitudinal, in-plane shear-wave and out-of-plane shear wave passbands. The acoustic wave velocities of the selected piezoelectric, at certain wafers (because the acoustic wave velocity has directional dependency), are based on the results of section 2. The geometrical characteristics of this type of metamaterials include lattice parameter, and inclusion ratios were chosen in order to ensure the existence and bandwidth of the complete band gap at certain frequency regimes. The filling fraction is based on the mechanical quality factor and the electromechanical coupling coefficient. While the electromechanical coupling coefficient increases by PZT volume fraction, the mechanical quality factor decreases, and at

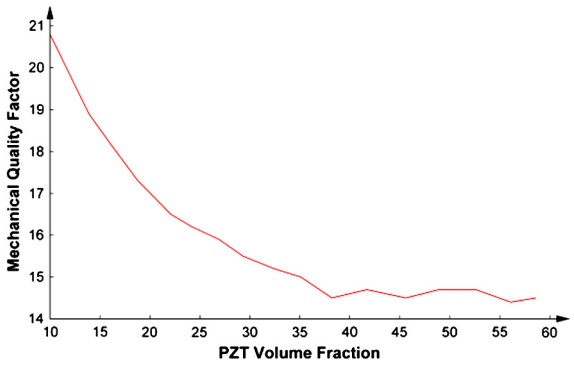

Fig. 7. The PZT volume fraction in terms of the mechanical quality factor.

range of 40% to 60%, the electromechanical coupling factor is stable, and the mechanical quality factor is slightly changed at the same volume fraction, so volume fraction range was selected as 40% to 60%.

To study the effect of the lattice parameter on band gap width, the lattice parameter was chosen as the variable, and the bandwidth variation was measured. The geometrical characteristics of this type of metamaterials include lattice parameter and inclusion ratios (at the selected range based on electromechanical coupling coefficient and the mechanical quality factor simultaneously) were chosen in order to ensure the existence and bandwidth of complete band gap at ultrasonic regime.

5. Fabrication method

Numerical analysis determines the technical specification of metamaterial, but the 3D printing method is suggested to achieve the sufficient fabrication accuracy and customize the product based on the required tolerances. A 3D printer, using the desired raw material, and the required blueprint, manufactures any desired object with the specifications and design of our choice with high-definition functional prototypes, which verifies the validity of the process. The piezoelectric columns are embedded in the honeycomb structure, which is made of resin and is constructed according to the method of 3D printing. The ProJet® 3510 SD with the resin material VisiJet® M3 Crystal can be used. The resolution at 32 μm is suggested and piezoelectric rods are inserted manually and combined by epoxy adhesion. The upper and bottom surfaces are to be polished after curing, and then the gold was sputtered on the two faces of elements and the package will be shielded.

6. Analysis results and discussion

Fig. 8 represents the complete band gap using the “reduced wave vector over frequency” method for acoustic pressure field and for all types of waves supported by rods (i.e. longitudinal, in-plane and out-of-plane wave) where it leads to a dispersion relation for these types of mechanical metamaterial consisting of lithium niobate piezoelectric scatters embedded in an air matrix. The geometrical parameter of phononic crystal and the dimension of piezoelectric rods are based on the electromechanical coupling coefficient, and the mechanical quality factor and the impedance spectra were taken into account (i.e. filling fraction 52%) for square lattice.

The blue line shows the location of a band gap based on the Brillouin zone. The acoustic wave velocity for piezoelectric rods was calculated based on the modified Christoffel’s equation provided in Figs. 2 (a), (b), and (c) that incorporate the electromechanical coupling effect and anisotropy. The acoustic wave velocity in the air was assumed to be 340 m/s and the density for air was assumed to be 0.001225 g/cm^3.

Since any propagated acoustic wave through the rods has three associated waves (i.e. longitudinal, in-plane wave, and out-of-plane wave), and all these types of waves have full band gap in this frequency range (i.e. from 8 to 10 kHz), Fig. 8 shows that no type of acoustic wave in this range can propagate through this metacomposite.

Studying the reliability, the width of the band gap is investigated. As the broad band devices that work over a large frequency domain have a commercial interest, Fig. 9 shows that the width of the band gap is changed by changing the PZT volume fraction (i.e. the filling fraction). Using the filling fractions 0.64 and 0.52, the forbidden band was enlarged from 8–10 kHz to 6.5–11 kHz. The crystal cut determines the properties of the crystal and affects the mode of vibration, frequency stability, acoustic wave velocity, aging; other manufacturing parameters were selected based on the figure of merit and the filling fraction. The filling fraction is based on the electromechanical coupling coefficient and the mechanical quality factor simultaneously.

7. Conclusions

The acoustic wave velocity supported by piezoelectric rods was represented by using the modified Christoffel equation to demonstrate the efficiency of the suggested metamaterial, especially in the ultrasonic regime. The electromechanical coupling effect and anisotropy were taken into account in this equation.

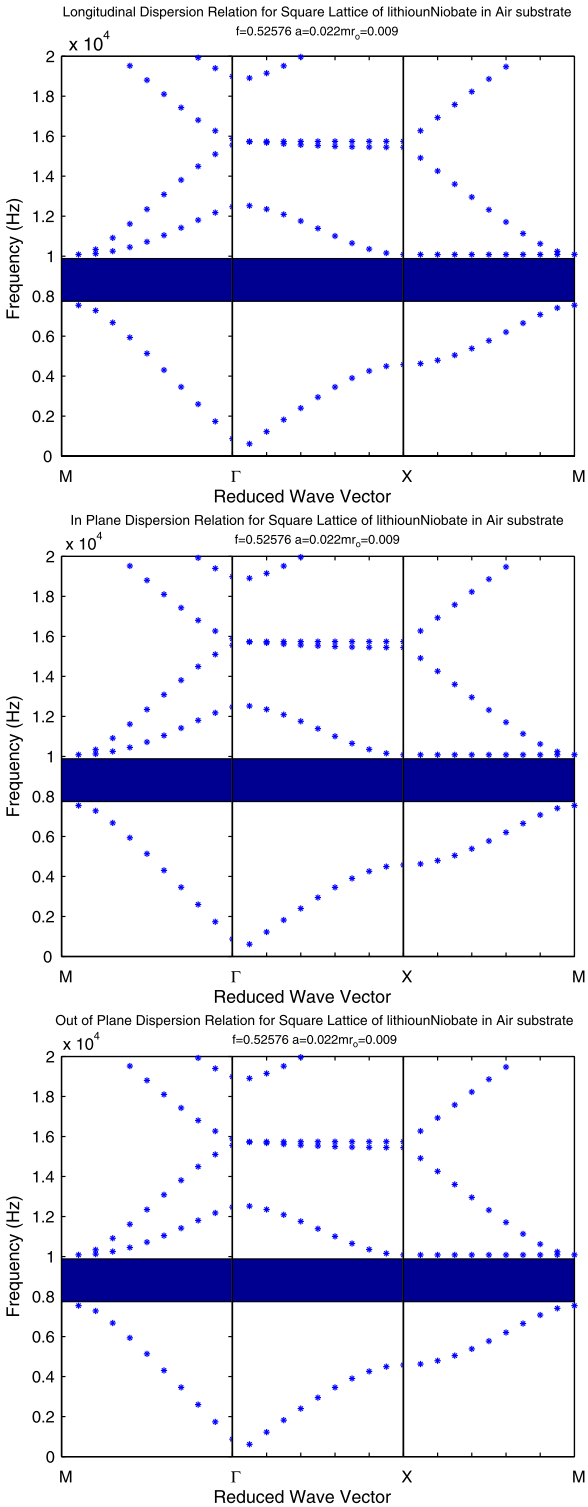

Fig. 8. Dispersion relations of a phononic crystal consisting of "Y-cut" wafers lithium niobate rods, embedded in an air background (filling fraction: 52%) for a square lattice, where the blue line shows the location of a band gap, based on the Brillouin zone.

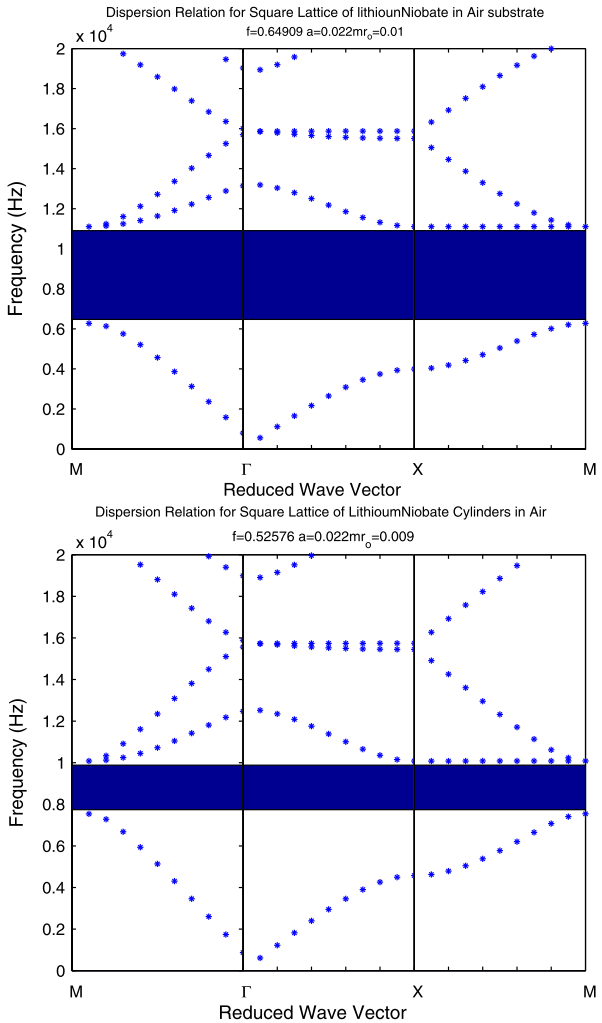

Fig. 9. The dispersion relation of square lattice of "Y-cut" lithium niobate piezoelectric cylinders embedded in air with filling fractions of 0.64 and 0.52, respectively.

Using the utilized modified PWEM in conjunction with "Bloch–Floquet" theorem, the acoustic wave equation with acoustic pressure field was applied rather than the displacement; the complete band gap was achieved by the contrast between acoustic wave velocities at rods and inclusion. The acoustic wave velocity contrast between the rods and substrate, and the density ratio between inclusion and host are critical for band gap range.

Using the impedance spectra of the piezoelectric rod and the electromechanical coupling coefficient and mechanical quality factor in terms of PZT volume fraction, the filling factor was determined, and a stable and balanced point from both factors' points of view is necessary.

To demonstrate the efficiency of the full band gap for wafers of piezoelectric devices as well as for one type of geometry and specific PZT volume fraction range, and every type of wave (i.e. longitudinal, in-plane wave and out-of-plane wave), the full band gap are represented.

The proposed ultrasonic phononic crystal system showed the feasibility of using phononic crystal systems to mitigate ultrasonic noise but at the expense of PZT volume fraction range and size. Despite of limitations in the range for increasing the size, this type of meta-composite is a suitable candidate for elastic wave control, especially to mitigate industrial noise at ultrasonic regime with reasonable size and complete band gap where they can also be used as omnidirectional acoustic wave guides that are used for long distance communication in the infrasound satellite-based wireless communication industry, or on-chip filters because in low-frequency ultrasonic regime, other technologies are too large for this type of application.

Because of the high contrast in all types of velocities ($\frac{c_{\text{Rod}}}{c_{\text{Air}}} \approx [45–73]$) and mass density ($\frac{\rho_{\text{Rod}}}{\rho_{\text{Air}}} \approx 14$), the corresponding huge impedance (i.e. $z_i = \rho_i c_i$) of the plane wave contrast ($\frac{z_1}{z_2} \approx 1043$) between air and rods impedes the penetration of acoustic wave inside the rods and, then, the effect of transversal waves can be fully disregarded, so the curves coincide in this case.

The omnidirectional property of this type of metamaterial that the forbidden band gap has no dependency on wave direction is a key property for excellent performance over traditional one or metamaterials with partial band gap.

The dependency of the band-gap-to-lattice parameter and the filling fraction means that these metamaterials are tunable, and that tunability is controlled by lattice parameter and filling fraction variation, or that these metamaterials are waveguides and have the selectivity of the frequency property.

When faster control is required, electro-optic modulators are good candidates. But, very high voltages are necessary, whereas acousto-optic modulators are much faster and have low power consumption. So these piezoelectric-based acoustic metamaterials are pioneers toward infrasound communication for long distances with low power consumption and faster control.

Finally, since the plane wave expansion method, associated with the "Bloch–Floquet" theorem, relies on the Fourier transform, the limitation of the Fourier transform is inherited; in other words, it does not include the location information that consequently has difficulty in representing transient states, especially with large acoustic mismatch. In this case, a wavelet-based method that has location and frequency is recommended.

Acknowledgements

This work was supported by University of Tehran Laboratories. The authors acknowledge the assistance of Donya Ravid from NORTECH Engineering and Research Corp., and of Mohammad Reza Mottian with some of the graphic arts and supports; They would like to show their gratitude to Fatima Rezaei and Zahra Rezaei for the language service.

Appendix A

The wave equation is:

$$\nabla \cdot \left[\frac{1}{\rho(\tilde{\mathbf{r}})} \nabla p(\tilde{\mathbf{r}}) \right] + \frac{\omega^2}{\rho(\tilde{\mathbf{r}}) c^2(\tilde{\mathbf{r}})} p(\tilde{\mathbf{r}}) = 0 \tag{30}$$

where $c(\tilde{\mathbf{r}})$ and $\rho(\tilde{\mathbf{r}})$ are the sound speed and mass density respectively and are modulated by the periodic structures and $p(\tilde{\mathbf{r}})$ is the acoustic pressure field.

(It is possible to obtain a simpler set of the displacement equation by introducing the scalar and vector potentials such that:

$$\mathbf{u} = \nabla \mathbf{\Phi} + \nabla \times \mathbf{H}$$

The resolution of a vector field into the gradient of a scalar field and the curl of a zero-divergence vector is due to a theorem by Helmholtz [50].

Since the plane of polarization is parallel to the cavity axis, it is recalled that SH waves do not undergo mode conversion, then the resultant displacement and stress fields will be governed by a scalar potential (Eq. (31)).)

The wave equation can be rewritten using a scalar potential $\Phi(\tilde{\mathbf{r}}, t)$ in such a way that $\rho \tilde{\mathbf{u}} = \nabla \Phi(\tilde{\mathbf{r}}, t)$ [51] where

$$\frac{1}{\rho c_l^2} \frac{\partial^2 \Phi}{\partial t^2} = \nabla \cdot \left(\rho^{-1} \nabla \Phi \right) \tag{31}$$

means that $\frac{1}{\rho c_l^2}$ is the longitudinal elastic constant.

Since the acoustic pressure field has the Bloch form, so:

$$p(\tilde{\mathbf{r}}) = \mathrm{e}^{\mathrm{i}(\tilde{\mathbf{k}}) \cdot (\tilde{\mathbf{r}}) - \omega t} \sum_{(\tilde{\mathbf{G}})} \phi_{\tilde{\mathbf{k}}}(\tilde{G}) \mathrm{e}^{\mathrm{i}(\tilde{\mathbf{G}}) \cdot (\tilde{\mathbf{r}})} \tag{32}$$

Based on the Bloch theorem, the mass density and sound speed can be expanded by a discrete plane wave, also $\alpha(\tilde{\mathbf{G}})$ and $\beta(\tilde{\mathbf{G}})$ are determined from an inverse Fourier transform:

$$\frac{1}{p(\tilde{\mathbf{r}})} = \sum_{(\tilde{\mathbf{G}})} \alpha(\tilde{\mathbf{G}}) \mathrm{e}^{\mathrm{i}(\tilde{\mathbf{G}}) \cdot (\tilde{\mathbf{r}})} \tag{33}$$

$$\frac{1}{\rho(\tilde{\mathbf{r}}) c^2(\tilde{\mathbf{r}})} p(\tilde{\mathbf{r}}) = \sum_{(\tilde{\mathbf{G}})} \beta(\tilde{\mathbf{G}}) \mathrm{e}^{\mathrm{i}(\tilde{\mathbf{G}}) . (\tilde{\mathbf{r}})} \tag{34}$$

By substituting the Bloch forms into the wave equation and the expanded wave equation into the initial wave equation, one has:

$$\sum_{(\tilde{\mathbf{G}})} \left[\alpha\left((\tilde{\mathbf{G}}) - (\tilde{\mathbf{G}}')\right)\left((\tilde{\mathbf{k}}) + (\tilde{\mathbf{G}})\right) \cdot \left((\tilde{\mathbf{k}}) + (\tilde{\mathbf{G}}')\right) - \beta\left((\tilde{\mathbf{G}}) - (\tilde{\mathbf{G}}')\right)\omega^2 \right] \alpha_{(\tilde{\mathbf{G}})(\tilde{\mathbf{G}}')} = 0 \tag{35}$$

By a finite number of Fourier components (N), the dispersive relation is achieved [52,53].

$$\sum_{(\tilde{\mathbf{G}})} \Gamma_{(\mathbf{G}),(\tilde{\mathbf{G}}')} \phi_{\tilde{\mathbf{k}}}(\tilde{G}') = 0 \tag{36}$$

$$-\det[\Gamma_{(\mathbf{G}),(\tilde{\mathbf{G}}')}] = \det\left[\alpha\left((\tilde{\mathbf{G}}) - (\tilde{\mathbf{G}}')\right)\left((\tilde{\mathbf{k}}) + (\tilde{\mathbf{G}})\right) \cdot \left((\tilde{\mathbf{k}}) + (\tilde{\mathbf{G}}')\right) - \beta\left((\tilde{\mathbf{G}}) - (\tilde{\mathbf{G}}')\right)\omega^2\right]_{(\tilde{\mathbf{G}}),(\tilde{\mathbf{G}}')} = 0 \tag{37}$$

The acoustic wave velocities that rods can support are determined from a modified Christoffel equation.

Here, the system consists of piezoelectric rods that have density ρ_{rod} and fill fraction f, with a circular cross-section embedded air background with density ρ_{air}. Then:

$$\begin{aligned} \rho(\tilde{\mathbf{G}}) &= \rho_{\text{rod}}^{-1} f + \rho_{\text{air}}^{-1}(1-f) \equiv \overline{\rho^{-1}}, \qquad \tilde{\mathbf{G}} = 0 \\ \rho(\tilde{\mathbf{G}}) &= \left(\rho_{\text{rod}}^{-1} - \rho_{\text{air}}^{-1}\right) F(\tilde{\mathbf{G}}) \equiv \Delta\rho^{-1} F(\tilde{\mathbf{G}}), \quad \tilde{\mathbf{G}} \neq 0 \end{aligned} \tag{38}$$

$$F(\tilde{\mathbf{G}}) = A_{\text{c}}^{-1} \int_{A_{\text{c}}} \mathrm{d}^2\mathbf{r} \mathrm{e}^{-\mathrm{j}\tilde{\mathbf{G}}\cdot\mathbf{r}} \tag{39}$$

and the structure factor for this type of system is defined in the PWEM as:

$$F(\tilde{\mathbf{G}}) = 2f \frac{J_1(\mathrm{G}r_0)}{\mathrm{G}r_0} \tag{40}$$

where J_1 is the first-kind Bessel function of first order.

The square lattice configuration has a reciprocal lattice vector defined in the PWE method as:

$$\tilde{\mathbf{G}} = \left(\frac{2\pi}{a}\right)(n_1 x_1 + n_2 x_2) \tag{41}$$

References

[1] B. Smagowska, M. Pawlaczyk-Łuszczyńska, Effects of ultrasonic noise on the human body—a bibliographic review, Int. J. Occup. Saf. Ergon. 19 (2) (2013) 195–202.
[2] J.D. Joannopoulos, S.G. Johnson, J.N. Winn, et al., Photonic Crystals: Molding the Flow of Light, Princeton University Press, Princeton, NJ, USA, 2011.
[3] Y. Pennec, B. Djafari-Rouhani, J.O. Vasseur, et al., Tunable filtering and demultiplexing in phononic crystals with hollow cylinders, Phys. Rev. E, Stat. Nonlinear Soft Matter Phys. 69 (4) (2004) 46608, http://dx.doi.org/10.1103/PhysRevE.69.046608.
[4] C.M. Soukoulis, Photonic Crystals and Light Localization in the 21st Century, Springer, 2001.
[5] E.L. Thomas, Opportunities in Protection Materials Science and Technology for Future Army Applications, Wiley Online Library, 2011.
[6] M. Sigalas, E.N. Economou, Band structure of elastic waves in two dimensional systems, Solid State Commun. 86 (3) (1993) 141–143.
[7] M. Kushwaha, P. Halevi, L. Dobrzynski, et al., Acoustic band structure of periodic elastic composites, Phys. Rev. Lett. 71 (13) (1993) 2022–2025, http://dx.doi.org/10.1103/PhysRevLett.71.2022.
[8] Y. Ding, Z. Liu, C. Qiu, et al., Metamaterial with simultaneously negative bulk modulus and mass density, Phys. Rev. Lett. 99 (9) (2007) 93904.
[9] A. Bergamini, T. Delpero, L. De Simoni, et al., Phononic crystal with adaptive connectivity, Adv. Mater. 26 (9) (2014) 1343–1347.
[10] M. Torres, F. Montero de Espinosa, D. García-Pablos, et al., Sonic band gaps in finite elastic media: surface states and localization phenomena in linear and point defects, Phys. Rev. Lett. 82 (15) (1999) 3054–3057, http://dx.doi.org/10.1103/PhysRevLett.82.3054.
[11] M. Kafesaki, M.M. Sigalas, N. García, Frequency modulation in the transmittivity of wave guides in elastic-wave band-gap materials, Phys. Rev. Lett. 85 (19) (2000) 4044–4047, http://dx.doi.org/10.1103/PhysRevLett.85.4044.
[12] A. Khelif, B. Djafari-Rouhani, J. Vasseur, et al., Transmission and dispersion relations of perfect and defect-containing waveguide structures in phononic band gap materials, Phys. Rev. B 68 (2) (2003) 24302, http://dx.doi.org/10.1103/PhysRevB.68.024302.
[13] T. Miyashita, Full band gaps of sonic crystals made of acrylic cylinders in air – numerical and experimental investigations, Jpn. J. Appl. Phys., Part 1, Reg. Pap. Short Notes Rev. Pap. 41 (5S) (2002) 3170–3175, http://stacks.iop.org/1347-4065/41/i=5S/a=3170.
[14] A. Khelif, A. Choujaa, S. Benchabane, et al., Guiding and bending of acoustic waves in highly confined phononic crystal waveguides, Appl. Phys. Lett. 84 (22) (2004) 4400–4402.
[15] A. Khelif, B. Djafari-Rouhani, J. Vasseur, et al., Transmittivity through straight and stublike waveguides in a two-dimensional phononic crystal, Phys. Rev. B 65 (17) (2002) 174308, http://dx.doi.org/10.1103/PhysRevB.65.174308.
[16] Y. Pennec, B. Djafari-Rouhani, J.O. Vasseur, et al., Acoustic channel drop tunneling in a phononic crystal, Appl. Phys. Lett. 87 (26) (2005) 261912.
[17] T. Gorishnyy, C.K. Ullal, M. Maldovan, et al., Hypersonic phononic crystals, Phys. Rev. Lett. 94 (11) (2005) 115501, http://dx.doi.org/10.1103/PhysRevLett.94.115501.
[18] A.S. Phani, J. Woodhouse, N.A. Fleck, Wave propagation in two-dimensional periodic lattices, J. Acoust. Soc. Am. 119 (4) (2006) 1995–2005.
[19] M.N. Armenise, C.E. Campanella, C. Ciminelli, et al., Phononic and photonic band gap structures: modelling and applications, Phys. Proc. 3 (1) (2010) 357–364, http://resolver.scholarsportal.info/resolve/18753892/v03i0001/357_papbgsmaa.
[20] J.Y. Yeh, Control analysis of the tunable phononic crystal with electrorheological material, Physica B, Condens. Matter 400 (1–2) (2007) 137–144, http://www.sciencedirect.com/science/article/pii/S0921452607004796.
[21] J.-F. Robillard, O.B. Matar, J.O. Vasseur, et al., Tunable magnetoelastic phononic crystals, Appl. Phys. Lett. 95 (12) (2009), http://scitation.aip.org/content/aip/journal/apl/95/12/10.1063/1.3236537.
[22] L.-Y. Wu, M.-L. Wu, L.-W. Chen, The narrow pass band filter of tunable 1D phononic crystals with a dielectric elastomer layer, Smart Mater. Struct. 18 (1) (2009) 15011, http://stacks.iop.org/0964-1726/18/i=1/a=015011.
[23] M. Ruzzene, A.M. Baz, Attenuation and localization of wave propagation in periodic rods using shape memory inserts, in: SPIE's 7th Annual International Symposium on Smart Structures and Materials, 2000, pp. 389–407.
[24] Y.-Z. Wang, F.-M. Li, W.-H. Huang, et al., Wave band gaps in two-dimensional piezoelectric/piezomagnetic phononic crystals, Int. J. Solids Struct. 45 (14–15) (2008) 4203–4210, http://linkinghub.elsevier.com/retrieve/pii/S0020768308001017.

[25] X.-Y. Zou, Q. Chen, B. Liang, et al., Control of the elastic wave bandgaps in two-dimensional piezoelectric periodic structures, Smart Mater. Struct. 17 (1) (2008) 15008, http://stacks.iop.org/0964-1726/17/i=1/a=015008.
[26] J. Zhao, Y. Pan, Z. Zhong, Theoretical study of shear horizontal wave propagation in periodically layered piezoelectric structure, J. Appl. Phys. 111 (6) (2012), http://scitation.aip.org/content/aip/journal/jap/111/6/10.1063/1.3694801.
[27] S.-E. Park, T.R. Shrout, Characteristics of relaxor-based piezoelectric single crystals for ultrasonic transducers, IEEE Trans. Ultrason. Ferroelectr. Freq. Control 44 (5) (1997) 1140–1147.
[28] E. Sun, W. Cao, W. Jiang, et al., Complete set of material properties of single domain $0.24Pb(In_{1/2}Nb_{1/2})O_3–0.49Pb(Mg_{1/3}Nb_{2/3})O_3–0.27PbTiO_3$ single crystal and the orientation effects, Appl. Phys. Lett. 99 (3) (2011) 32901–32903, http://www.ncbi.nlm.nih.gov/pmc/articles/PMC3155577/.
[29] J.P. Dowling, M. Scalora, M.J. Bloemer, et al., Photonic bandgap apparatus and method for delaying photonic signals, Google Patents, 1998.
[30] S. Johnson, J. Joannopoulos, Block-iterative frequency-domain methods for Maxwell's equations in a planewave basis, Opt. Express 8 (3) (2001) 173–190, http://www.opticsexpress.org/abstract.cfm?URI=oe-8-3-173.
[31] M. Collet, M. Ouisse, M. Ruzzene, et al., Floquet–Bloch decomposition for the computation of dispersion of two-dimensional periodic, damped mechanical systems, Int. J. Solids Struct. 48 (20) (2011) 2837–2848, http://www.sciencedirect.com/science/article/pii/S0020768311002125.
[32] Y. Wang, W. Song, E. Sun, et al., Tunable passband in one-dimensional phononic crystal containing a piezoelectric $0.62Pb(Mg_{1/3}Nb_{2/3})O_3–0.38PbTiO_3$ single crystal defect layer, Phys. E 60 (2014) 37–41, http://www.sciencedirect.com/science/article/pii/S1386947714000526.
[33] N. Jalili, Piezoelectric-Based Vibration Control: From Macro to Micro/Nano Scale Systems, Springer Science & Business Media, 2009.
[34] K. Haisch, M.Z. Atashbar, B.J. Bazuin, Identification of acoustic wave modes in piezoelectric substrates, in: 2005 IEEE International Conference on Electro Information Technology, 2005, p. 5.
[35] R. McIntosh, A.S. Bhalla, R. Guo, Finite element modeling of acousto-optic effect and optimization of the figure of merit, in: Proc. SPIE 8497, Photonic Fiber and Crystal Devices: Advances in Materials and Innovations in Device Applications VI, October 15, 2012, p. 849703.
[36] R. McIntosh, Directional Dependence of Acousto-Optic Figure of Merit, http://demonstrations.wolfram.com/DirectionalDependenceOfAcoustoOpticFigureOfMerit/, Wolfram Demonstrations Project, Published: February 13, 2013.
[37] R.E. Newnham, Properties of Materials: Anisotropy, Symmetry, Structure, Oxford University Press, Oxford, UK, 2005.
[38] Y. Pennec, J.O. Vasseur, B. Djafari-Rouhani, et al., Two-dimensional phononic crystals: examples and applications, Surf. Sci. Rep. 65 (8) (2010) 229–291.
[39] M.S. Kushwaha, P. Halevi, G. Martínez, et al., Theory of acoustic band structure of periodic elastic composites, Phys. Rev. B 49 (4) (1994) 2313–2322.
[40] F. Meseguer, M. Holgado, D. Caballero, et al., Rayleigh-wave attenuation by a semi-infinite two-dimensional elastic-band-gap crystal, Phys. Rev. B 59 (19) (1999) 12169–12172.
[41] R. Antos, M. Veis, Fourier Factorization in the Plane Wave Expansion Method in Modeling Photonic Crystals, INTECH Open Access Publisher, 2012.
[42] M. Wilm, S. Ballandras, V. Laude, et al., A full 3D plane-wave-expansion model for 1-3 piezoelectric composite structures, J. Acoust. Soc. Am. 112 (3) (2002) 943–952.
[43] M.M. Sigalas, E.N. Economou, Elastic and acoustic wave band structure, J. Sound Vib. 158 (2) (1992) 377–382.
[44] Y.Y. Chen, Z. Ye, Theoretical analysis of acoustic stop bands in two-dimensional periodic scattering arrays, Phys. Rev. E, Stat. Nonlinear Soft Matter Phys. 64 (3) (2001) 36616, http://dx.doi.org/10.1103/PhysRevE.64.036616.
[45] Y.-Y. Chen, Z. Ye, Acoustic attenuation by two-dimensional arrays of rigid cylinders, Phys. Rev. Lett. 87 (18) (2001) 4, http://arxiv.org/abs/cond-mat/0101442.
[46] Y. Cao, Z. Hou, Y. Liu, Convergence problem of plane-wave expansion method for phononic crystals, Phys. Lett. A 327 (2–3) (2004) 247–253, http://www.sciencedirect.com/science/article/pii/S0375960104007029.
[47] V. Laude, M. Wilm, S. Benchabane, et al., Full band gap for surface acoustic waves in a piezoelectric phononic crystal, Phys. Rev. E, Stat. Nonlinear Soft Matter Phys. 71 (3) (2005) 36607, http://dx.doi.org/10.1103/PhysRevE.71.036607.
[48] J.O. Vasseur, B. Djafari-Rouhani, L. Dobrzynski, et al., Complete acoustic band gaps in periodic fibre reinforced composite materials: the carbon/epoxy composite and some metallic systems, J. Phys. Condens. Matter 6 (42) (1994) 8759.
[49] R. McIntosh, Impedance Spectra of Piezoelectric Rods, http://demonstrations.wolfram.com/ImpedanceSpectraOfPiezoelectricRods/, Wolfram Demonstrations Project, Published: March 20, 2014.
[50] K.F. Graf, Wave Motion in Elastic Solids, Ohio State University Press, Columbus, 1975.
[51] D.P. Elford, L. Chalmers, G.M. Swallowe, et al., Vibrational Modes of Slotted Cylinders, European Acoustics Association/Slovenian Acoustical Society/Alps Adria Acoustics Association, 2010.
[52] T. Miyashita, Sonic crystals and sonic wave-guides, Meas. Sci. Technol. 16 (5) (2005) R47–R63.
[53] D.P. Elford, L. Chalmers, F.V. Kusmartsev, et al., Matryoshka locally resonant sonic crystal, J. Acoust. Soc. Am. 130 (5) (2011) 2746–2755.